

Absence of Translational Symmetry Breaking in Nonmagnetic Insulator Phase on Two-Dimensional Lattice with Geometrical Frustration

Shinji Watanabe and Masatoshi Imada

Institute for Solid State Physics, University of Tokyo, 5-1-5, Kashiwanoha, Kashiwa, Chiba 277-8581

(Received March 22, 2024)

The ground-state properties of the two-dimensional Hubbard model with nearest-neighbor and next-nearest-neighbor hoppings at half filling are studied by the path-integral-renormalization-group method. The nonmagnetic-insulator phase sandwiched by the paramagnetic-metal phase and the antiferromagnetic-insulator phase shows evidence against translational symmetry breaking of the dimerized state, plaquette singlet state, staggered flux state, and charge ordered state. These results support that the genuine Mott insulator which cannot be adiabatically continued to the band insulator is realized generically by Umklapp scattering through the effects of geometrical frustration and quantum fluctuation in the two-dimensional system.

KEYWORDS: nonmagnetic insulator, geometrical frustration, Mott transition, two-dimensional Hubbard model, path integral renormalization group method (PIRG)

The Mott transition between the metallic and insulating states has been a subject of general interest in condensed matter physics.¹⁾ Many intensive studies have been done to clarify the nature of the Mott transition by employing analytical and numerical methods.²⁾ The present understanding on the Mott transition is that almost all the Mott insulators have translational symmetry breakings such as AF ordering and dimerization in the ground state with only a few exceptions.²⁾ When the translational symmetry is broken, the Brillouin zone is folded so that the even number of electrons is contained in the unit cell.³⁾ These cases may be adiabatically continued to the band insulator by the band-gap formation, and may not belong to the class of the genuine Mott insulator which has the odd number of electrons in the unit cell.

For theoretical models, an exception of the Mott insulator without Brillouin zone folding is found in the ground state of the one-dimensional Hubbard model at half filling, where neither symmetry breaking nor spin excitation gap exists.⁴⁾ The absence of symmetry breaking in the ground state implies that a highly quantum-mechanical state is realized. Then, the following question arises: Does the Mott insulator without translational symmetry breaking exist except in one-dimensional systems? This has been a long-standing problem since Anderson's proposal in 70's.⁵⁾ He originally considered a spin-1/2 model on the triangular lattice, which may realize the genuine Mott insulator by the combined effects of strong magnetic frustration and quantum fluctuation, although there exists an argument for the presence of a magnetic long-ranged order in this system.^{6,7)} Recently, the Hubbard model on an isotropic triangular lattice has been studied. It shows the presence of the nonmagnetic-insulator (NMI) phase near the boundary of the metal-insulator transition.⁸⁾

In this letter, we consider the Hubbard model on square lattice (HMSL) with nearest and next-nearest neighbor hoppings at half filling as a candidate for the genuine Mott insulator. Effects of geometrical frustration (see Fig. 1(a)) and quantum fluctuation are expected to induce highly quantum-mechanical effects in this system. Recent weak-coupling renormalization group study suggests possible mechanism of insulating gap formation through Umklapp scattering without any translational symmetry breaking.⁹⁾ Recent path-integral-renormalization-group (PIRG) study has clearly shown the presence of an insulating phase without magnetic long-range order in intermediate to strong-coupling regime.¹⁰⁾ It is crucially important to fully understand the nature of the nonmagnetic Mott insulator phase and also the metallic phase near the metal-insulator boundary. We study various correlation functions to get insight into this problem. Our results support that the nonmagnetic-insulator phase does not show apparent translational symmetry breaking near the band-width-control Mott transition.

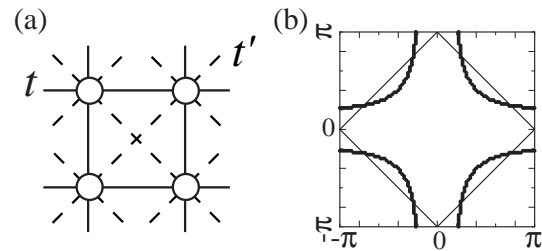


Fig. 1. (a) Lattice structure of the two-dimensional Hubbard model on square lattice with transfer t and t' . (b) Fermi surface for $t = 1$, $t^0 = 0.5$ and $U = 0.0$ at half filling on $N = 100 \times 100$ lattice (filled circle) and magnetic Brillouin zone (solid line).

The H M SL we consider is

$$H = \sum_{\langle i,j \rangle} t_{ij} c_i^\dagger c_j + \sum_i U n_i n_{i\uparrow}; \quad (1)$$

where c_i (c_i^\dagger) is the annihilation (creation) operator on the i -th site with spin and $n_i = c_i^\dagger c_i$ in the N -site system. The transfer integral is taken as $t_{ij} = t$ for the nearest-neighbor sites and $t_{ij} = t^0$ for the next-nearest-neighbor sites. Throughout this letter, we take t as energy unit and consider the half-filled case, $\sum_i n_i = N/2$.

We have applied the PIRG method^{11,12} to eq. (1). This algorithm starts from and improves the mean-field Hartree-Fock solution by increasing the dimension of truncated Hilbert space in non-orthogonal basis optimized by the path-integral operation. A variance extrapolation of improved wave function has been taken to reach the true ground state of finite systems in a controlled way. This method does not have difficulties as in previous methods such as the negative sign problem in the quantum Monte Carlo calculations. The PIRG calculations have been done in the system up to $N = 12 \times 12$ lattices under the periodic boundary condition.

First we discuss the change of the Fermi surface (FS). The FS can be defined by the \mathbf{q} points where the momentum distribution $n(\mathbf{q}) = \frac{1}{2N} \sum_{i,j} \langle c_i^\dagger c_j \rangle e^{i\mathbf{q} \cdot (\mathbf{R}_i - \mathbf{R}_j)}$ exhibits a sharp discontinuity. We show the contour plots of $\langle c_i^\dagger c_j \rangle$ in Fig. 2 (a) to estimate the FS for $t = 1$ and $t^0 = 0.5$ on the $N = 12 \times 12$ lattice. The large values of $\langle c_i^\dagger c_j \rangle$ specify the possible location of the FS in the momentum space. We see that $\langle c_i^\dagger c_j \rangle$ has larger values around $\mathbf{q} = (\pm 2; \pm 2)$ than those around $\mathbf{q} = (0; 0)$ and $(\pm 2; 0)$. This indicates that renormalization of electrons occurs around both ends of the arc of the FS more prominently rather than around the center of the arc. Although it is difficult to demonstrate the validity of the Luttinger's theorem within the present analysis due to the finite-size effects, we note that there exists the following tendency concerning the shape of the FS: As U increases, the FS around $\mathbf{q} = (\pm 2; \pm 2)$ tends to expand to the $\mathbf{q} = (0; 0)$ point and the FS around the ends of the arc tends to shrink to the $\mathbf{q} = (0; 0)$ and $(\pm 2; 0)$ points. This can be also seen from the contour plots of $n(\mathbf{q})$ in Fig. 2 (b) $U = 3.5$, (c) $U = 4.0$ and (d) $U = 7.5$. The large values of $\langle c_i^\dagger c_j \rangle$ roughly correspond to the yellow area of the contour plot of $n(\mathbf{q})$ as seen from Fig. 2 (a) and Fig. 2 (c). The metal-insulator transition is estimated at $U_{c1} = 4.75 \pm 0.25$ by the calculations of charge gap and double occupancy, and the antiferromagnetic transition specified by vector $\mathbf{Q} = (\pm 2; 0)$ in spin correlation function, $S(\mathbf{q}) = \frac{1}{2N} \sum_{i,j} \langle S_i S_j \rangle e^{i\mathbf{q} \cdot (\mathbf{R}_i - \mathbf{R}_j)}$; is estimated at $U_{c2} = 7.25 \pm 0.25$.¹⁰ Although the FS does not exist in the insulator phase, we also show here the contour plot of $n(\mathbf{q})$ in the antiferromagnetic-insulator (AFI) phase in Fig. 2 (d) to see the tendency of the deformation of the contour line of the Fermi level. From Figs. 2 (b)–(d), we see that the FS deforms from the $U = 0$ FS toward the magnetic Brillouin zone specified by the vector \mathbf{Q} , which are represented as the filled circles and the solid line, respectively in Fig. 1 (b). Namely, the FS deforms

toward the perfect nesting as U increases. This tendency has been predicted by the renormalization-group study on the H M SL in the weak-coupling regime.¹³

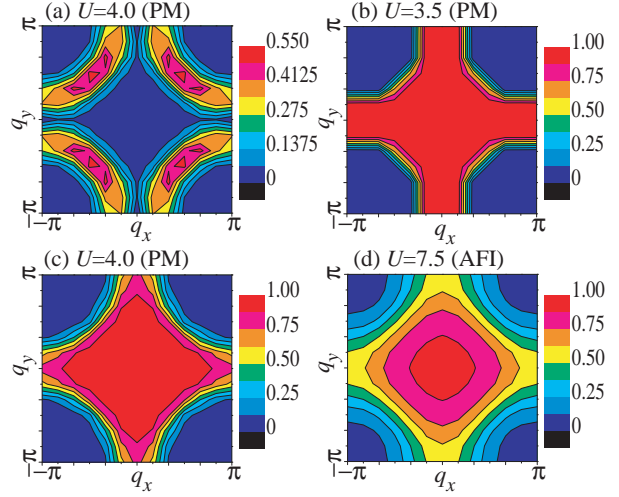


Fig. 2. Contour plots of $\langle c_i^\dagger c_j \rangle$ for (a) $U = 4.0$ and $n(\mathbf{q})$ for (b) $U = 3.5$, (c) $U = 4.0$, and (d) $U = 7.5$ for $t = 1$, $t^0 = 0.5$ on the $N = 12 \times 12$ lattice at half filling. PM and AFI represent paramagnetic metal and antiferromagnetic insulator, respectively.

Next we discuss the nature of the NM I phase. In the NM I phase for $U_{c1} < U < U_{c2}$, $S(\mathbf{q})$ has broad peaks at incommensurate positions shifted from $\mathbf{q} = (\pm 2; 0)$ toward $\mathbf{q} = (0; 0)$ and $(\pm 2; 0)$ directions, in contrast to the AFI phase for $U > U_{c2}$ with the commensurate peak at $\mathbf{q} = \mathbf{Q}$.¹⁰ A remaining question to be clarified is whether some other translational symmetry is broken, or not in the NM I phase. To examine the nature of the NM I phase let us consider the $U \rightarrow \infty$ limit of the phase diagram. In the strong-correlation limit, the H M SL becomes the J_1 - J_2 Heisenberg model in the leading order: $H = J_1 \sum_{\langle i,j \rangle} S_i S_j + J_2 \sum_{\langle\langle i,j \rangle\rangle} S_i S_j$; where hi and fg represent the nearest-neighbor sites and next-nearest-neighbor sites, respectively. Here, $J_1 = 4t^2/U$ and $J_2 = 4t^0/U$ are both antiferromagnetic interactions so that magnetic frustration arises. For $J_2 = J_1 < 0.4$ the Neel order with peak structure in $S(\mathbf{q})$ at $\mathbf{q} = (\pm 2; 0)$ was proposed while for $J_2 = J_1 > 0.6$ the collinear order with $\mathbf{q} = (0; 0)$ or $(\pm 2; 0)$ peak in $S(\mathbf{q})$ was proposed. However, as for the intermediate region of $0.4 < J_2 = J_1 < 0.6$, no definite conclusion has been drawn on the nature of the ground state: The possibility of the columnar dimerized state^{14,15} (see Fig. 3 (a)), the plaquette singlet state¹⁶ (see Fig. 3 (b)) and the resonating-valence-bond¹⁷ state was discussed. The AFI and the NM I phases found in the H M SL can be connected to the Neel-ordered and the NM phases of the J_1 - J_2 Heisenberg model, respectively, in the limit $U \rightarrow \infty$. Therefore, the NM I phase in the phase diagram of the H M SL could have some connection to the region $0.4 < J_2 = J_1 < 0.6$.

We first note that it is in principle hard to prove the existence of the genuine Mott insulator because it is difficult

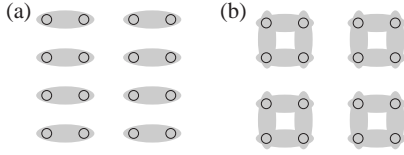


Fig. 3. Schematic pictures of (a) the columnar-dimerized state and (b) the plaquette-singlet state.

cult to prove the absence of all the possible translational symmetry breakings. To get insight into this problem, we examine every symmetry breaking ever proposed, which is likely to occur in the NM I phase.

To examine the possibility of the dimerized state and the plaquette state, we have calculated the dimer-correlation function D_{ij} for $i, j = x, y$ defined by $D_{ij} = \langle O_i O_j \rangle$; where $O_i = \frac{1}{N} \sum_{i=1}^N (1)^i S_i \cdot \hat{S}_i$, and \hat{S}_i represents the unit vector in the $(=x \text{ or } y)$ direction. Figure 4 shows the system-size dependence of D_{xx} for $t^0 = 0.5$, and $U = 0.0, 3.5, 4.5, 5.0, 5.7$ and 8.0 on the $N = 4, 6, 8, 10, 12$ lattices. We note that the dimer correlation is enhanced in comparison with $U = 0$ results and it indicates that short-ranged correlation develops. The extrapolated values of D_{xx} to the thermodynamic limit, however, seem to vanish for all interaction strength calculated here. These results indicate that the columnar-dimerized state and the plaquette-singlet state (see Fig. 3) proposed as a candidate for the NM I phase with broken translational symmetry are not realized in the present system. The D_{xy} correlations have about 2- or 3-orders of magnitude smaller values than the D_{xx} correlations for each system size and the extrapolation to the thermodynamic limit also shows no realization of the D_{xy} -type ordering.

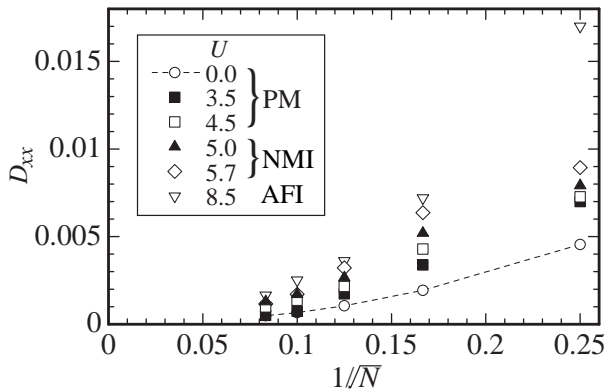


Fig. 4. The system-size dependence of the dimer-correlation functions for $t = 1.0$, $t^0 = 0.5$ and $U = 0.0$ (open circle), 3.5 (filled square), 4.5 (open square), 5.0 (filled triangle), 5.7 (open diamond) and 8.5 (open triangle) at half filling on $N = 4, 6, 8, 10, 12$ lattices.

Next, we examine symmetry breaking of various density waves proposed in the literature.¹⁸⁾ We calculate

the current-correlation function defined by

$$C_{\alpha\beta}(q) = J_{\alpha\beta}(q) J^Y(q);$$

where $J_{\alpha\beta}(q) = \frac{1}{N} \sum_{k, l} c_{k, \alpha}^{\dagger} c_{k+q, \beta} f_l(k)$, with $f_1(k) = \cos(k_x) + \cos(k_y)$, $f_2(k) = \cos(k_x) - \cos(k_y)$, $f_3(k) = 2 \cos(k_x) \cos(k_y)$, and $f_4(k) = 2 \sin(k_x) \sin(k_y)$.

Among finite q , we have confirmed that the peak structure in $C_{\alpha\beta}(q)$ for $\alpha = 1, 2, 3$ and 4 appears at $q = (\pi; \pi) = Q$ for $t^0 = 0.5$, and $U = 0.0, 3.5, 4.5$, and 5.7 . Here $C_2(Q)$ corresponds to the so-called staggered- π state¹⁸⁾ (see inset of Fig. 5(b)). Figure 5 shows the system-size dependence of $J_{\alpha\beta}(Q)$ for $t^0 = 0.5$, and $U = 0.0, 3.5, 4.5$ and 5.7 on the $N = 4, 6, 8, 10, 12$ and 12×12 lattices. If the long-ranged order of these types occurs, $J_{\alpha\beta}(Q)$ should have a finite value in the thermodynamic limit. Although $J_{\alpha\beta}(Q)$ for $\alpha = 1$ and 2 are enhanced in comparison with $U = 0$ results, all current correlations calculated here seem to vanish for $N \rightarrow \infty$ and the correlations remain short ranged. These results suggest that the symmetry breaking specified by the order parameter, $J_{\alpha\beta}(q)$ for $\alpha = 1, 2, 3, 4$ does not occur in the NM I phase.

We have also calculated the charge-correlation function defined by

$$N(q) = \frac{1}{N} \sum_{i, j} (n_i n_j - \langle n_i \rangle \langle n_j \rangle) e^{iq \cdot (R_i - R_j)};$$

with $n_i = \sum_{\alpha} c_{i, \alpha}^{\dagger} c_{i, \alpha}$. We show $N(q)$ in Fig. 6 for (a) $U = 0.0$, (b) 4.5, (c) 5.0, and (d) 5.7 for $t^0 = 0.5$ on the $N = 12 \times 12$ lattice. No conspicuous peak structure develops even in the NM I phase such as $U = 5.0$ and 5.7 . Figure 7 shows the system-size dependence of $N(Q) = N$, for $t^0 = 0.5$, and $U = 0.0, 3.5, 4.5, 5.0$ and 5.7 on the $N = 4, 6, 8, 10, 12$ and 12×12 lattices. The extrapolation of maximum values of $N(q)$ to $N \rightarrow \infty$ goes to zero for all interaction strength calculated here. The absence of prominent peak structure in $N(q)$ in various system sizes excludes the possibility of incommensurate charge orderings. Thus, we conclude that the charge order does not occur in the NM I phase.

In summary, we have studied the ground-state properties of the Hubbard model on the square lattice with nearest-neighbor and next-nearest-neighbor hoppings at half filling by using the PRG method. We show that the renormalization of electrons occurs in the metallic phase drastically around $q = (0; \pi)$ and $(\pi; 0)$ rather than around $q = (\pi; \pi)$. There exists a tendency that the Fermi surface deforms toward the magnetic Brillouin zone as U increases, namely, toward the perfect nesting. In the nonmagnetic-insulator phase sandwiched by the paramagnetic-metal and the antiferromagnetic-insulator phases, the calculations of dimer-, current-, and charge-correlation functions show no evidence of symmetry breakings such as the columnar-dimerized state, plaquette-singlet state, staggered- π state (d-density-wave state), s-density-wave state, and charge-ordered

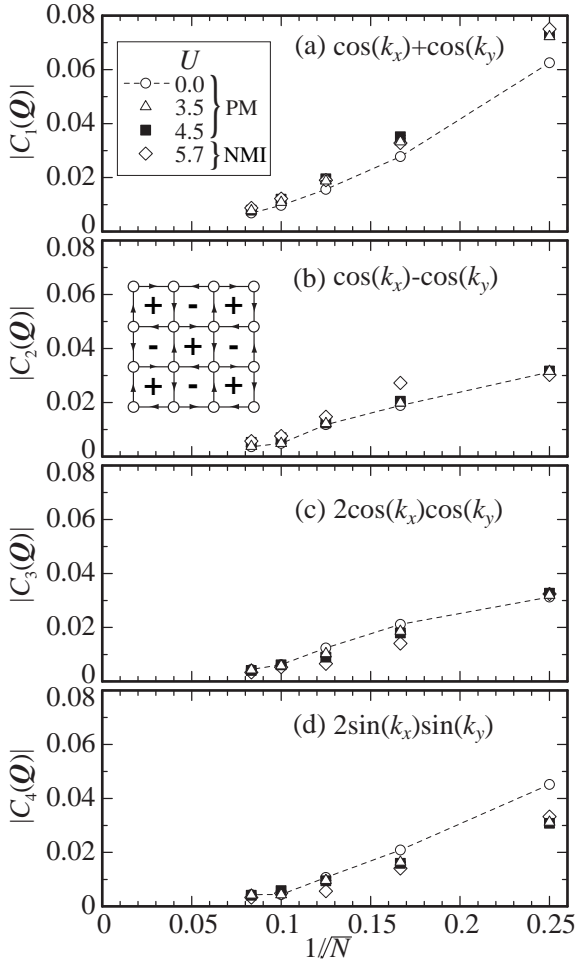


Fig. 5. The system-size dependence of current correlations $|C_i(Q)|$ at $Q = (\pi/2, \pi/2)$ with (a) $f_1 = \cos(k_x) + \cos(k_y)$ (b) $f_2 = \cos(k_x) - \cos(k_y)$, (c) $f_3 = 2\cos(k_x)\cos(k_y)$, and (d) $f_4 = 2\sin(k_x)\sin(k_y)$ for $t = 1.0$, $t^0 = 0.5$ and $U = 0.0$ (open circle), 3.5 (open triangle), 4.5 (filled square) and 5.7 (open diamond) at half filling on $N = 4, 6, 8, 10, 12$ lattices. Inset of (b) illustrates schematic picture of the staggered flux state.

state. Although a possibility of some other symmetry breakings cannot be excluded, our results support that the Mott insulator without translational symmetry breaking is realized in the nonmagnetic-insulator phase, where the translational symmetry breakings undergo quantum melting. This implies that the genuine Mott insulator which can not be adiabatically continued to the band insulator is realized by Umklapp scattering via the effects of geometrical frustration and quantum fluctuation near the metal-insulator phase boundary.

We thank S. Sachdev for discussions. The work is supported by the Research for the Future program from the Japan Society for the Promotion of Science under grant number JSPS-RFTF97P01103. A part of our computation has been done at the supercomputer center in the Institute for Solid State Physics, University of Tokyo.

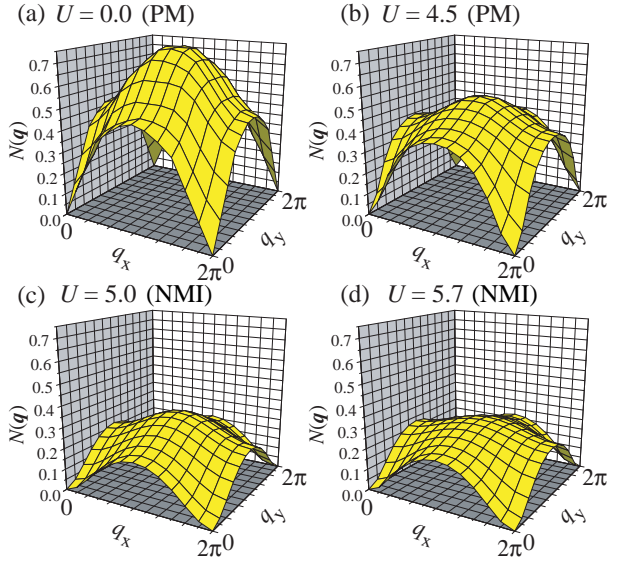


Fig. 6. The charge correlation functions for $t = 1.0$, $t^0 = 0.5$, and (a) $U = 0.0$, (b) 4.5, (c) 5.0 and (d) 5.7 at half filling on the $N = 12 \times 12$ lattice.

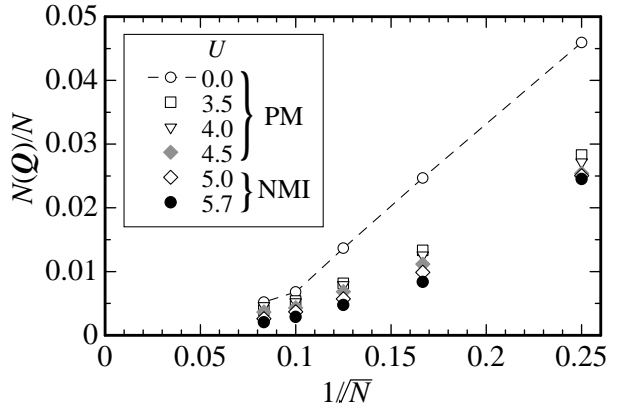


Fig. 7. The system-size dependence of the peak value of charge correlation functions for $t = 1.0$, $t^0 = 0.5$ and $U = 0.0$ (open circle), 3.5 (open square), 4.0 (open triangle), 4.5 (filled diamond), 5.0 (open diamond) and 5.7 (filled circle) at half filling on $N = 4, 6, 8, 10, 12$ lattices.

- 15) O. P. Sushkov, J. Oitmaa and Z. Weihong: Phys. Rev. B 63 (2001) 104420.
- 16) M. E. Zhitomirsky and K. Ueda: Phys. Rev. B 54 (1996) 9007.
- 17) L. Capriotti, et al.: Phys. Rev. Lett. 27 (2001) 97201.
- 18) I. A. Aleshchuk and J. B. Marston: Phys. Rev. B 37 (1988) 3774.